http://dx.doi.org/10.5012/bkcs.2012.33.10.3331

Particle Size Effect: Ru-Modified Pt Nanoparticles Toward Methanol Oxidation

Sechul Kim,[†] Ting Zhang,[‡] Jin-Nam Park,[§,*] Choong Kyun Rhee,[†,‡,*] and Hojin Ryu[#]

[†]*Gruaduate School of Analytical Science and Technology, Chungnam National University, Daejeon 305-704, Korea*
[*]*E-mail: ckrhee@cnu.ac.kr*
[‡]*Department of Chemistry, Chungnam National University, Daejeon 305-704, Korea*
[§]*Department of New & Renewable Energy, Kyungil University, Gyeongbuk 712-701, Korea. [*]E-mail: jnpark@kiu.ac.kr*
[#]*Energy Materials Research Center, Korea Research Institute of Chemical Technology, Daejeon 305-600, Korea*
Received June 9, 2012, Accepted July 13, 2012

Ru-modified Pt nanoparticles of various sizes on platelet carbon nanofiber toward methanol oxidation were investigated in terms of particle size effect. The sizes of Pt nanoparticles, prepared by polyol method, were in the range of 1.5-7.5 nm and Ru was spontaneously deposited by contacting Pt nanoparticles with the Ru precursor solutions of 2 and 5 mM. The Ru-modified Pt nanoparticles were characterized using transmission electron microscopy, X-ray photoelectron spectroscopy and cyclic voltammetry. The methanol oxidation activities of Ru-modified Pt nanoparticles, measured using cyclic voltammetry and chronoamperometry, revealed that when the Pt particle size was less than 4.3 nm, the mass specific activity was fairly constant with an enhancement factor of more than 2 at 0.4 V. However, the surface area specific activity was maximized on Pt nanoparticles of 4.3 nm modified with 5 mM Ru precursor solution. The observations were discussed in terms of the enhancement of poison oxidation by Ru and the population variation of Pt atoms at vertices and edges of Pt nanoparticles due to selective deposition of Ru on the facets of (111) and (100).

Key Words : Ruthenium, Platinum, Particle size effect, Methanol oxidation, Spontaneous deposition

Introduction

The development of fuel cells with high energy efficiency and low environmental pollution is globally interested due to the elevated concerns about sustainable energy. The major advantages of fuel cell are the production of clean energy and high power generation efficiency by electrochemical oxidation of fuels.[1,2] Direct methanol fuel cell (DMFC) is one of promising portable power sources, because methanol is a fuel easier to handle than hydrogen. To be practical in power generation, however, methanol has a barrier to be overcome because the rate of methanol oxidation is lower than that of hydrogen. Therefore, development of efficient electrochemical catalysts toward methanol oxidation is an important issue in commercialization of DMFC. Currently, PtRu black is widely used for the anode of DMFC, in which Ru is known to enhance the resistivity of Pt to CO-type catalytic poisons.[3]

Particle size effect of electrochemical Pt catalysts has been investigated seriously. A decrease in particle size certainly increases the surface area available for electrochemical reactions. As the particle size decreases, on the other hand, the areas of Pt facets on nanoparticles such as (111) and (100) decrease, and the numbers of Pt atoms of low coordination numbers at edges and vertices increase.[4] This particular change associated with the crystallography of Pt nanoparticle may lead to change in electrocatalytic activity. For example, CO adsorption becomes stronger as particle size decreases (thus, CO oxidation potential shifts in the positive direction). Meanwhile, formation of OH available to CO oxidation becomes feasible for the same reason to enhance the CO oxidation.[5] These examples demonstrate that the size effect is a complicate but important subject to be understood. Another example is a volcano plot for oxygen reduction reaction: as the particle size decreases, the surface area specific activity decreases, and the surface area increases to show a volcano plot of mass specific activity.[6] On the other hand, our recent studies on the oxidation of methanol and formic acid on Pt nanoparticles[7] and Bi-modified Pt nanoparticles[8] demonstrated that the surface area specific activities of the two organic molecules remained fairly constant although Pt nanoparticle size decreased, most likely due to the two previously-mentioned effects of CO adsorption and OH formation operating in the opposite directions. Therefore, the size effect of electrocatalysts may depend on electrochemical reactions under investigation.

Ru is an important ingredient for electrochemical Pt catalysts for methanol oxidation. During methanol oxidation on Pt surfaces, CO-type catalytic poisons form to reduce the methanol oxidation rate by hampering further methanol adsorption. In the presence of Ru on Pt surfaces, the Ru is oxidized at a more negative potential than Pt to provide oxygen-containing species such as OH as revealed by our scanning tunneling microscopic work.[9] Various methods to modifying Pt surfaces with Ru have been reported: alloying,[10-13] electrochemical deposition,[14-16] vacuum deposition,[17,18] and spontaneous deposition.[19-22]

In this work, we report particle size effect in methanol oxidation observed on Ru-modified Pt nanoparticles supported on platelet carbon nanofiber (PCNF). The separate

issues of the size effect of Pt nanoparticles in methanol oxidation and the modification of Pt with Ru were combined all together. The size effect of Ru-modified Pt nanoparticles in methanol oxidation is discussed along with various characteristics including effective surface area and atomic ratio of the two elements as well as electrochemical behavior.

Experimental

Materials. Pt nanoparticles on PCNF were prepared using polyol method.[23] The particle size of Pt was controlled by adjusting the pH value of ethylene glycol reducing medium as detailed in ref. 7. The obtained particle sizes were 7.5, 6.0, 4.3, 3.6, 2.5, and 1.5 nm. The loading amount of Pt, as determined by quantifying the residues (PtO_2) after burning off the carbon support in air, was 10 wt % regardless of particle size. The PCNF was obtained from Kyushu University, Japan.[24-27]

Modification of Pt nanoparticles was performed using spontaneous deposition.[28] The Ru precursor solutions of 2 and 5 mM was obtained by dissolving appropriate amounts of $RuCl_3 \cdot xH_2O$ (99.9%, Wako, Japan) in 0.1 M $HClO_4$ (70%, ACS reagent, Sigma-Aldrich, USA). The spontaneous deposition procedure of Ru was as follows: (i) adding 0.05 g of Pt nanoparticles on PCNF into a Ru precursor solution, (ii) stirring for 10 h, (iii) removing Ru-modified Pt nanoparticles on PCNF from the precursor solution and washing thoroughly, (iv) reducing electrochemically the Ru species adsorbed on Pt nanoparticles at 0 V (*versus* Ag/AgCl) for 30 min, and (v) filtering, washing, drying, and grinding.[8]

Characterization. Sizes of Pt nanoparticles were estimated by measuring diameters of more than 150 Pt nanoparticles in transmission electron microscope (TEM) images, obtained using an instrument (JEM-2010F, JEOL). A quantitative and qualitative analysis was performed using an X-ray photoelectron spectrometer (XPS, Thermo Electron Co., MultiLab 2000, USA). In the XPS analysis, an Mg Kα X-ray beam (1253.6 eV) was utilized as an excitation source and a multichannel hemispherical electron energy analyzer operated at constant pass energy of 15 eV. The observed spectra were curve-fitted using a mixed Gaussian-Lorentzian line shape and Shirley baselines.

Electrochemical Measurements. A conventional three-electrode system was employed using a potentiostat (Bipotentiostat, AFCBP1, Pine). Specifically, the counter electrode was a Pt gauze (25 mm × 25 mm, 52 mesh, Φ = 0.1 mm, Johnson Matthey, USA), and the reference electrode was a homemade Ag/AgCl electrode in 1.0 M NaCl solution. The potentials reported in this work were against the reference electrode. An Au rotating disk electrode, embedded in a Teflon holder and rotated at a rotating speed of 1000 rpm, was used to eliminate the CO_2 bubbles formed during methanol oxidation.

A paste of Ru-modified Pt nanoparticles on PCNF was prepared by mixing 0.025 g of catalyst powder, 5 g of deionized water, and 0.05 g of Nafion (5 wt %, Wako, Japan). After sonication of the paste for 30 min, 20 μL of the paste was spread onto the Au disk and dried under an IR lamp for 30 min to be ready for electrochemical measurements.

The aqueous working solution for methanol oxidation was 2.0 M methanol (99.8+%, HPLC grade, Johnson Matthey, London, U. K.) + 0.5 M H_2SO_4 (95-97%, Merck, German). All solutions in electrochemical cell were purged with nitrogen (99.9%) before electrochemical experiments.

Results and Discussion

Characterization of Pt Nanoparticles. Figure 1 shows typical TEM images of Pt nanoparticles on PCNF. The reason for the employment of PCNF as support was that the graphite-edge-exposing surface of PCNF would avoid possible complicate problems associated with carbon supports of high surface area such as Vulcan. The Pt nanoparticles were distributed homogenously on PCNF supports, and the sizes of the dispersed Pt nanoparticles were fairly

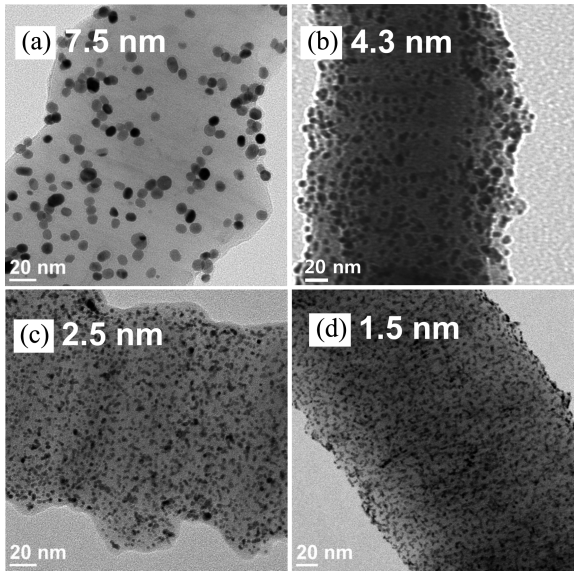

Figure 1. TEM images of Pt nanoparticles on PCNF (10 wt % Pt). The sizes of Pt particles are (a) 7.5 nm, (b) 4.3 nm, (c) 2.5 nm, and (d) 1.5 nm.

Table 1. Characteristics of Ru-modified Pt nanoparticles on PCNF

Particle size[a] (nm)	Surface area[b] (m^2/g)	Ru/Pt atomic ratio[c]	
		Ru concentration of precursor solution	
		2 mM	5 mM
1.5 ± 0.3	83	0.22	0.32
2.5 ± 0.5	76	0.24	0.31
3.6 ± 0.9	64	0.26	0.31
4.3 ± 1.1	46	0.22	0.29
6.0 ± 0.5	38	0.24	0.28
7.5 ± 1.4	29	0.25	0.31

[a]Particle size of unmodified Pt nanoparticles. [b]Measured independently by stripping charges of adsorbed hydrogen and CO. [c]Determined by XPS analysis.

even. As the pH of ethylene glycol reducing medium of Pt precursors increased, the size of Pt nanoparticles decreased from 7.5 nm to 1.5 nm. This result implies that the polyol method is useful to control the Pt particle size in preparation of supported Pt electrode catalyst comparing with the precipitation method which needs careful adjustment of pH in a narrow range to control Pt particle size.[29] The sizes of the investigated Pt nanoparticles are summarized in Table 1 (The particle size distributions for the each TEM image in Figure 1 are shown in Supporting Information.).

The surface areas of Pt nanoparticles on PCNFs were measured using stripping charges of adsorbed hydrogen and CO. The cyclic voltammograms of Pt nanoparticles in 0.5 M H_2SO_4 solutions for stripping of hydrogen and CO are shown in Figures 2 and 4 (see below). The surface areas measured by the two independent methods were reasonably consistent within experimental uncertainty (< 5%). Certainly,

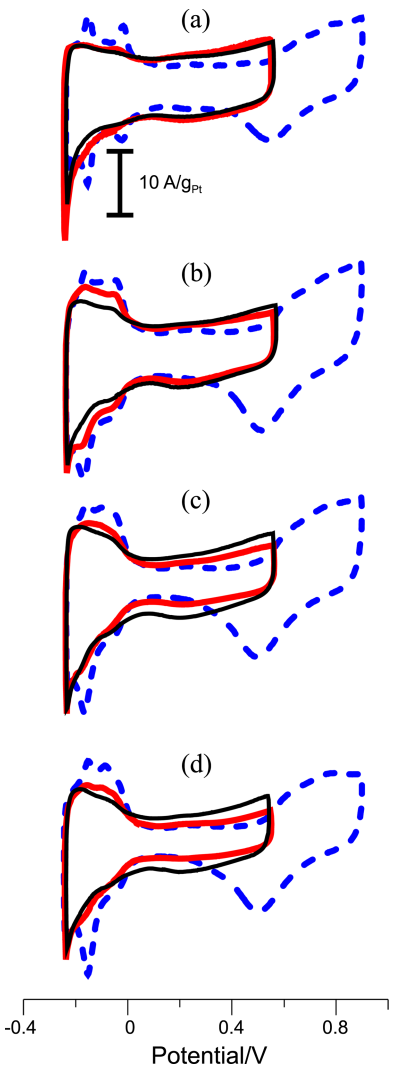

Figure 2. Cyclic voltammograms of Ru-modified Pt nanoparticles on PCNF in 0.5 M H_2SO_4 solution. The concentrations of Ru in Ru precursor solutions were 0 mM (blue dotted line), 2 mM (thick red solid line), and 5 mM (thin black solid line). The sizes of Pt particles were (a) 7.5 nm, (b) 4.3 nm, (c) 2.5 nm, and (d) 1.5 nm. Scan rate: 10 mV/s.

a decrease in particle size resulted in an increase in surface area as shown in Table 1. Our previous work revealed that the surface areas of Pt nanoparticles smaller than 2.5 nm were less than the theoretically calculated ones due to attachment of Pt nanoparticles to carbon support or aggregation of extremely small nanoparticles.[7]

Characterization of Ru-Modified Pt Nanoparticles. Figure 2 shows typical cyclic voltammograms of Ru-modified Pt nanoparticles on PCNF in 0.5 M H_2SO_4 solution. The voltammograms of unmodified Pt nanoparticles (dotted lines) clearly represent the characteristic features of polycrystalline Pt in 0.5 M H_2SO_4 solution. In particular, the charges related to the hydrogen region (−0.25 ~ 0.10 V) increased without any change in shape as the particle size decreased, indicating an increase in surface area. After spontaneous deposition of Ru, the voltammograms (solid lines) changed significantly. The charge of hydrogen region decreases, implying that the Pt surface was covered partially by spontaneously deposited Ru. The surface oxidation potential on the Ru-modified Pt nanoparticles shifted in the negative direction (*i.e.*, started roughly at 0.25 V, more negative than bare Pt by 0.2 V), indicating that Ru on Pt surfaces was easily oxidized. As the concentration of Ru precursor changed from 2 mM (thick red solid lines) to 5 mM (thin black solid lines), the features of Ru were more pronounced. The upper limit of potential scan of Ru-modified Pt nanoparticles was 0.6 V; at a higher potential, the deposited Ru dissolved.

Figure 3 is typical XPS spectra obtained from Pt nanoparticles of 1.5 nm on PCNF after spontaneous deposition of Ru in 5 mM Ru precursor solution followed by electrochemical reduction at 0 V for 30 min. The XPS spectra of Pt $4f_{7/2}$ (Figure 3(a)) revealed that Pt existed as mainly metallic Pt (71.4 eV) with slight amounts of PtO (72.7 eV) and PtO_2 (74.6 eV). The Ru spontaneously deposited on Pt nanoparticles was exclusively RuO_2 as judged with Ru 3p peaks at 462.9 and 485.3 eV (Figure 3(b)).[30] The existence of Pt and Ru oxides after electrochemical reduction of spontaneous deposition of Ru on Pt nanoparticles was certainly due to the oxidation of nanoparticle surfaces during the following procedures in air (See Experimental). The atomic ratios of Ru to Pt were estimated with the peaks of Pt $4f_{7/2}$ and Ru $3p_{3/2}$ using relative sensitivities of 2.55 and 1.30, respectively,[31] and tabulated in Table 1. Certainly, the amount of Ru was higher when the concentration of Ru in the precursor solution was higher. However, the amount of Ru did not depend on Pt particle size. The averages of Ru/Pt atomic ratio were 0.24 ± 0.02 and 0.30 ± 0.02 after spontaneous deposition in 2 and 5 mM Ru precursor solutions, respectively.

Oxidation of Adsorbed CO on Ru-Modified Pt Nanoparticles. Figure 4 shows the stripping voltammograms of adsorbed CO on Ru-modified Pt nanoparticles on PCNF. The adsorption of CO was carried out by contacting Pt nanoparticles on PCNF with CO-saturated 0.5 M H_2SO_4 solution for 15 min at 0 V, and the adsorbed CO was stripped oxidatively in CO-free 0.5 M H_2SO_4 solution. Regardless of Pt particle size, the stripping potential of CO on unmodified

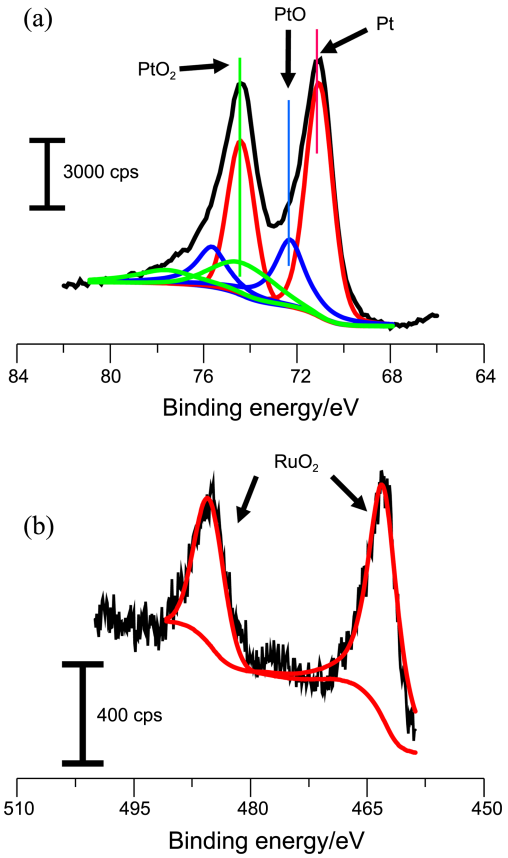

Figure 3. X-ray photoelectron spectra of Pt nanoparticles of 1.5 nm on PCNF modified with 5 mM Ru precursor solution: (a) Pt 4f and (b) Ru 3p.

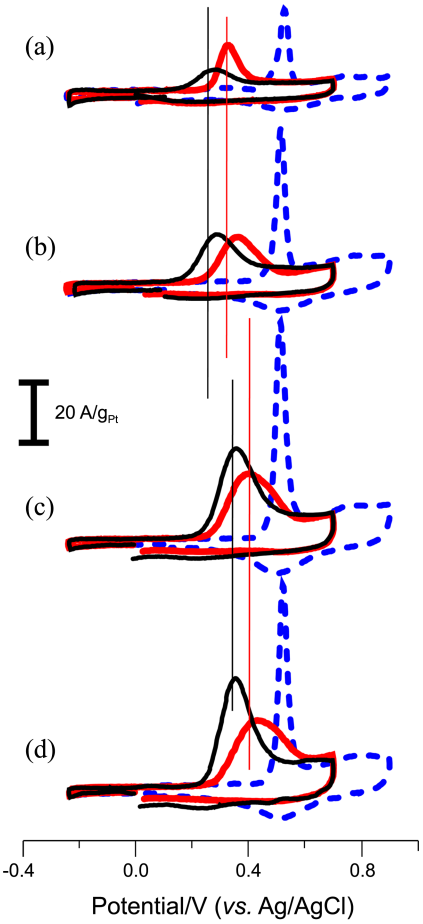

Figure 4. CO stripping voltammograms of Ru-modified Pt nanoparticles on PCNF in 0.5 M H_2SO_4 solution. The concentrations of Ru in Ru precursor solutions were 0 mM (blue dotted line), 2 mM (thick red solid line), and 5 mM (thin black solid line). The sizes of Pt particles were (a) 7.5 nm, (b) 4.3 nm, (c) 2.5 nm, and (d) 1.5 nm. The potential was measured against a Ag/AgCl electrode in 1.0 M NaCl solution. Scan rate: 10 mV/s.

Pt nanoparticles (dotted lines) was consistently 0.52 V, which has been interpreted as a combination of two oppositely affecting effects[9] (enhancement of OH formation and strong adsorption of CO with decreasing Pt particle size[32]). However, the stripping charges of CO were higher on smaller Pt nanoparticles, certainly due to an increase in the surface area of Pt nanoparticles. The presence of Ru induced CO stripping potential shift in the cathodic direction. When the particle size of Pt was 7.5 nm (Figure 4(a)), for example, the stripping potential shifted from 0.53 V to 0.32 V and further to 0.28 V upon modification with 2 and 5 mM Ru precursor solutions, respectively. On the other hand, as the Pt nanoparticle size decreased, the CO stripping potential on Ru-modified Pt nanoparticles shifted in the anodic direction. As indicated with solid vertical lines in Figure 4, the CO stripping potential observed on the Pt particles of 7.5 nm modified with 5 mM Ru precursor solution was 0.28 V, while that obtained on the Pt particles of 2.5 nm modified with the same precursor solution was 0.35 V. However, further cathodic shift was not observed on Ru-modified Pt nanoparticles of 1.5 nm. The potential shift of CO oxidation in the positive direction along with the decrease in particle size may be related to the distribution of surface atoms as a function of the particle size.[7] Specifically, the surface population of Pt atoms of low coordination numbers in cuboctahedral nanoparticles (*e.g.*, at vertices and edges) increases from 30% to 50% as the size decreases from 4.0 to 2.0 nm, while that of high coordination numbers (*e.g.*, in facets of (111) and (100)) decreases from 70% to 50% under the same size decrease. Because CO is known to strongly adsorb on Pt atoms at vertices and edges,[5] the anodic potential shift of CO oxidation implies that as particle size decreased, most of the adsorbed CO molecules were at the vertices and edges. If the Ru atoms are selectively deposited on the facets of (111) and (100), more Pt atoms at the vertices and edges would be exposed to CO as the Pt nanoparticles become smaller to cause the anodic potential shift of CO oxidation.

Oxidation of Methanol on Ru-Modified Pt Nanoparticles. Figure 5 shows the methanol oxidation voltammograms of Ru-modified Pt nanoparticles on PCNF in 2.0 M methanol + 0.5 M H_2SO_4 solution. On unmodified Pt nanoparticles (dotted lines), two oxidation peaks were observed at 0.62 V and 0.49 V during the anodic and cathodic scans, respectively. The shape of the methanol oxidation voltammogram did not depend on Pt nanoparticle size, although the oxida-

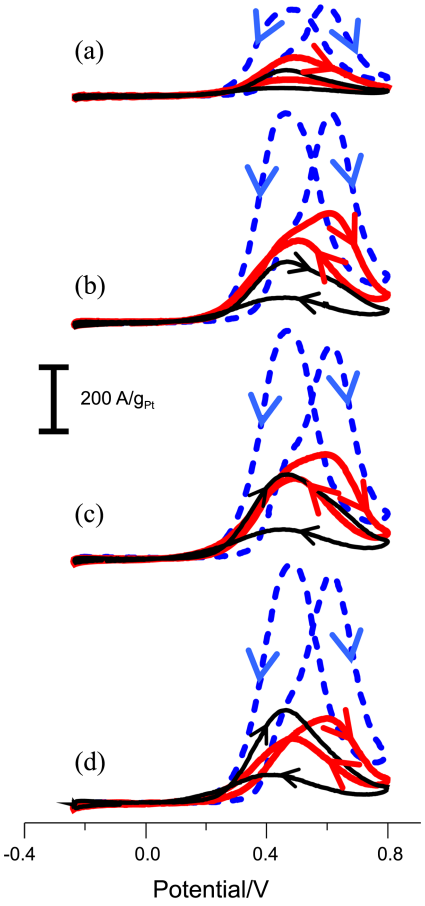

Figure 5. Cyclic voltammograms of Ru-modified Pt nanoparticles on PCNF in 2 M MeOH + 0.5 M H_2SO_4 solution. The concentrations of Ru in Ru precursor solutions were 0 mM (blue dotted line), 2 mM (thick red solid line), and 5 mM (thin black solid line). The sizes of Pt particles were (a) 7.5 nm, (b) 4.3 nm, (c) 2.5 nm, and (d) 1.5 nm. The potential was measured against a Ag/AgCl electrode in 1.0 M NaCl solution. Scan rate: 10 mV/s.

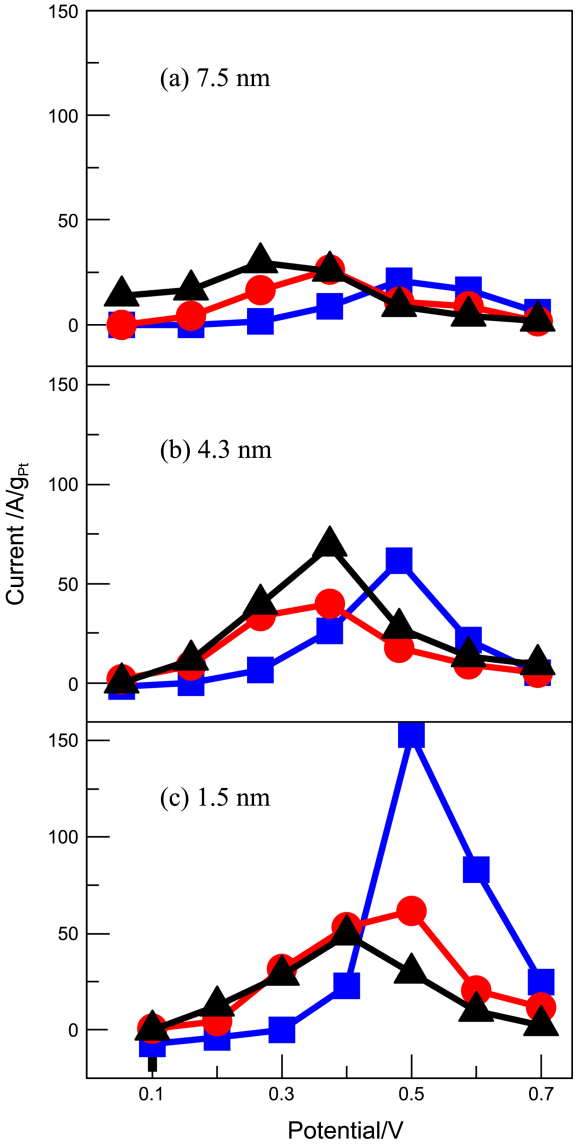

Figure 6. Potential-current plots of Ru-modified Pt nanoparticles on PCNF in 2 M MeOH + 0.5 M H_2SO_4 solution. The concentrations of Ru in Ru precursor solutions were (■) 0 mM, (●) 2 mM, and (▲) 5 mM. The current values were the chronoamperometric current measured after 30 min upon potential jump from −0.27 V to the specified potential under a rotating speed of 1000 rpm. The sizes of Pt particles were (a) 7.5 nm, (b) 4.3 nm, and (c) 1.5 nm. The potential was measured against a Ag/AgCl electrode in 1.0 M NaCl solution.

tion currents increased as Pt nanoparticle size decreased. On Ru-modified nanoparticles (solid lines), a few changes in methanol oxidation voltammogram were observed. The oxidation currents decreased in the presence of Ru, probably due to that the deposited Ru diminished the area of Pt surface effective for dissociative adsorption of methanol.[33] However, the peak potential of methanol oxidation especially in the anodic scan shifted remarkably from 0.62 V on unmodified Pt nanoparticles to 0.46 V on the nanoparticles modified with 5 mM Ru precursor solution (thin black solid lines). A comparison of the methanol oxidation voltammograms on Pt nanoparticles with different amounts of Ru (thin black and thick red solid lines in Figure 5) supports that more Ru caused more potential shift in the cathodic direction. On the other hand, the oxidation current curve during the cathodic scan was smaller than that observed during the anodic scan, and its potential did not shift significantly. These particular observations during cathodic scan are most likely related to the presence of Ru oxide species formed in the previous anodic scan. Thus, the Ru deposited on Pt nanoparticles certainly played dual roles in methanol oxidation: although it decreased the effective Pt surface area for methanol adsorption, it provided oxygenated species to facilitate oxidative removal of poisonous species from methanol. However, the employed voltammetric condition did not demonstrate particle size effect (see below).

Figure 6 is a plot of potential *versus* methanol oxidation chronoamperometric currents on Ru-modified Pt nanoparticles at the steady-states in 2.0 M methanol + 0.5 M H_2SO_4 solution. The presented currents were the currents observed at the steady-states (30 min) after a potential jump from −0.27 V to the aimed potentials under a rotating speed of 1000 rpm (not shown in this work). The onset potentials

on Ru-modified Pt nanoparticles are certainly and generally 0.2 V more negative than that on unmodified Pt nanoparticles. In addition, the potential of oxidation current maximum per unit mass of Pt on Ru-modified Pt nanoparticles, irrespective of particle size, was roughly 0.4 V, which is 0.1 V more negative than that on unmodified Pt nanoparticles. (It should be noted that the potential of oxidation current maximum on Pt nanoparticles of 1.5 nm modified with 2 mM Ru solution was 0.5 V rather than 0.4 V. This particular observation may imply a transient behavior from plain Pt surface to modified surface with a higher Ru content, which is not understood clearly. Because the particular current value was moderately reproducible within an experimental uncertainty (~10%), the Pt nanoparticles of 1.5 nm modified with 2 mM Ru solution would be exceptional.) However, the maximum current value strongly depends on particle size: as particle size decreases, the maximum current on unmodified Pt nanoparticles at 0.5 V exceeds that on Ru-modified Pt nanoparticles at 0.4 V. Specifically, when the particle size was 7.5 nm, the maximum current on Ru-modified Pt nanoparticles at 0.4 V (29 A/g) was slightly larger than that on unmodified particles at 0.5 V (21 A/g), while when the size was 1.5 nm, the maximum current on modified one at 0.4 V (53 A/g) was much smaller than that on unmodified one at 0.5 V (153 A/g). Therefore, the maximum methanol oxidation current per unit mass of Pt on Ru-modified Pt nanoparticles at 0.4 V strongly relies on the particle size of Pt, but the onset potential and maximum current potential do not depend on.

Figure 7 compares the variation of mass specific activity of Ru-modified nanoparticles with that of surface area specific activity of Ru-modified nanoparticles as a function of measured surface area of unmodified Pt nanoparticles. The mass specific activity and surface area specific activity were defined as the methanol oxidation chronoamperometric current at 0.4 V per unit mass of Pt and per unit surface area of unmodified Pt nanoparticles, respectively. The mass of Pt was 10% of the weight of the used powder of Pt nanoparticles on PCNF, regardless of particle size, while the surface areas were the measured ones listed in Table 1. The particle sizes of Pt nanoparticles corresponding to each studied surface area were indicated at the top of Figure 7 for clarity. The aim of the comparison is that mass specific activity is critical in practical applications, while surface area specific activity is crucial in understanding the electrocatalysis.

In Figure 7(a), it is quite clear that an increase in the amount of Ru deposits on Pt nanoparticles resulted in an enhancement of mass specific activity of Pt. When the size of Pt nanoparticles became smaller than 4.3 nm, the mass specific activities of Ru-modified Pt nanoparticles were more or less similar to each other considering an experimental uncertainty (~10%). The enhancement factor of mass specific activity was approximately more than 2, upon modification of Pt nanoparticles with 5 mM Ru precursor solution.

In Figure 7(b), the Pt nanoparticles of 4.3 nm modified

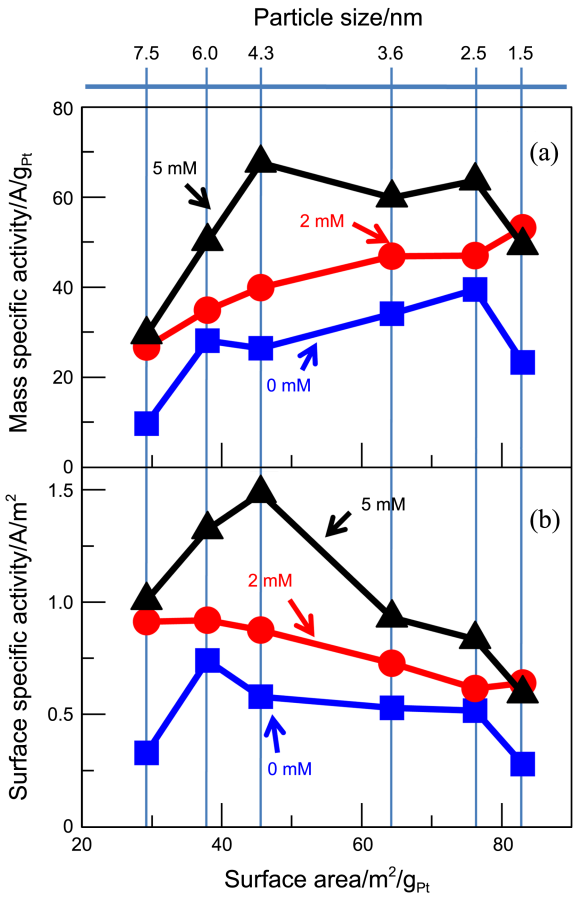

Figure 7. Plot of electrochemical methanol oxidation activities of Ru-modified Pt nanoparticles on PCNF *versus* surface area: (a) mass specific activities and (b) surface area specific activity. The currents are the currents at 0.4 V in Figure 6.

with 5 mM Ru precursor solution showed the highest surface area specific activity at 0.4 V among the investigated Ru-modified Pt nanoparticles. As the particle size decreased from 7.5 to 4.3 nm, the surface area specific activity increased significantly, especially on Pt nanoparticles modified with the 5 mM Ru precursor solution. Further decrease in particle size from 4.3 nm to 1.5 nm, however, resulted in a decrease in the surface area specific activity despite the inherent increase in Pt surface area. This particular observation may be related to the surface populations of Pt atoms at vertices and edges of nanoparticles.[7] When the particle size is larger than 4 nm, the population of Pt atoms of low coordination number increases slightly with the decrease in size. As the particles becomes smaller than 4 nm, on the other hand, the population of Pt atoms at vertices and edges increases rapidly. In the presence of Ru on Pt nanoparticles, smaller facets of (111) and (100) may be advantageous for methanol oxidation, so that the surface area specific activity increased along with the size decrease from 7.5 to 4.3 nm. As the facets become smaller, however, the increased number of Pt atoms at vertices and edges would hamper methanol oxidation by adsorbing poisonous species strongly. Here, it should be reminded that Ru deposited on the facets preferentially as implied by the anodic potential shift of CO

oxidation (Figure 4). The combination of the two particle size effects operating in the opposite direction in the presence of Ru would result in a maximum surface area specific activity on Pt nanoparticles of 4.3 nm, modified with 5 mM Ru precursor solution. Here, it should be recalled that Pt nanoparticles of 1.5 nm modified with 2 mM Ru solution is exceptional as discussed previously. In any circumstances, the mass specific activity of Ru-modified Pt nanoparticles smaller than 4.3 nm was fairly constant (Figure 7(a)) as a result of combination of increased surface area and reduced surface area specific activity, because the mass specific activity (A/g) is a product of surface area specific acidity (A/m^2) and surface area (m^2/g). Thus, Ru-modified Pt nanoparticles of 4.3-1.5 nm are appropriate for methanol oxidation in terms of practical mass activity.

Conclusions

The size effect of Ru-modified Pt nanoparticles of 7.5-1.5 nm in diameter has been investigated toward methanol oxidation. When Ru was spontaneously deposited onto Pt nanoparticles, the atomic ratio of Ru to Pt did not depend on particle size, but on the concentration of Ru in the precursor solutions. The chronoamperometric measurements revealed that the presence of Ru on Pt nanoparticles shifted the onset potential and current peak potential of methanol oxidation by 0.2 and 0.1 V, respectively, in the cathodic direction regardless of particle size, although the peak current strongly depended on the size. The mass specific activities measured with chronoamperometry were fairly constant when the Pt particle size was smaller than 4.3 nm, and the enhancement factor was more than 2. Contrastingly, the surface area specific activity was maximized on Pt nanoparticles of 4.3 nm modified with 5 mM Ru precursor solution. The differences in the dependencies of mass specific activity and surface area specific activity on Pt nanoparticle size were interpreted in terms of three effects of Ru-modified Pt nanoparticles related to particle size: (1) the inherent Pt surface area provided by Pt nanoparticles, (2) the enhancement of poison oxidation presented by Ru, and (3) the population variation of free Pt atoms at vertices and edges of nanoparticles due to selective deposition of Ru on the facets of (111) and (100).

Acknowledgments. This work was supported by the Energy & Resource Recycling of the Korea Institute of Energy Technology Evaluation and Planning (KETEP) grant funded by the Korea government Ministry of Knowledge Economy (2010501010006C). Sechul Kim was supported by Specialized Graduate School Program (2009-008146) through a National Research Foundation of Korea grant funded by the MEST.

Supporting Information. The particle size distributions for the each TEM image in Figure 1 are available at the BKCS website (http://www.kcsnet.or.kr/bkcs).

References

1. Ross P. N. In *Oxygen Reduction Reaction on Smooth Single Crystal Electrodes*; Vielstich, W., Lamm, A., Gasteiger, H. A., Eds.; John Wiley and Sons: 2003; Vol. 2, pp 465-480.
2. EG&G Technical Services *Fuel Cell Handbook*, 7th edn.; U.S. Department of Energy: 2004.
3. Ralph, T. R.; Hogarth, M. P. *Platinum Metals Rev.* **2002**, *46*, 117.
4. Kinoshita, K. *Electrochemical Oxygen Technology*; John Wiley and Sons: 1992.
5. Maillard, F.; Pronkin, S.; Savinova, E. R. In *Influence of Size on the Electrocatalytic Activities of Supported Metal Nanoparticles in Fuel Cell-Related Reactions*; Vielstich, W., Yokokawa, H., Gasteiger, H. A., Eds.; John Wiley and Sons: 2009; Vol. 5, pp 91-111.
6. Markovic, N. M.; Schmidt, T. J.; Stamenkovic, V.; Ross, P. N. *Fuel Cells* **2001**, *1*, 105.
7. Rhee, C. K.; Kim, B.-J.; Ham, C.; Kim, Y.-J.; Song, K.; Kwon, K. *Langmuir* 2**009**, *25*, 7140.
8. Jung, C.; Zhang, T.; Kim, B.-J.; Kim, J.; Rhee, C. K.; Lim, T.-H. *Bull. Korean Chem. Soc.* **2010**, *31*, 1543.
9. Jung, C.; Kim, J.; Rhee, C. K. *Electrochem. Comm.* **2010**, *12*, 1363.
10. Shukla, A. K.; Neegat, M.; Bera, P.; Jayaram, V.; Hegde, M. S. *J. Electroanal. Chem.* **2001**, *504*, 111.
11. Gasteiger, H. A.; Markovic, N.; Ross, P. N. *J. Phys. Chem.* **1995**, *99*, 16757.
12. Arico, A. S.; Antonucci, P. L.; Modica, E.; Baglio, V.; Kim, H.; Antonucci, V. *Electrochimica Acta* **2002**, *47*, 3723.
13. Holstein, W. L.; Rosenfeld, H. D. *J. Phys. Chem. B* **2005**, *109*, 2176.
14. Cramm, S.; Friedrich, K. A.; Geyzers, K.-P.; Stimming, U.; Vogel, R. *Fresen. J. Anal. Chem.* **1997**, *358*, 189.
15. Maillard, F.; Gloaguen, F.; Leger, J.-M. *J. Appl. Electrochem.* **2003**, *33*, 1.
16. Vigier, F.; Gloaguen, F.; Leger, J. M.; Lamy, C. *Electrochimica Acta* **2001**, *46*, 4331.
17. Hoster, H.; Iwasita, T.; Baumgartner, H.; Vielstich, W. *J. Electrochem. Soc.* **2001**, *148*, A496.
18. Davies, J. C.; Hayden, B. E.; Pegg, D. J.; Rendall, M. E. *Surf. Sci.* **2002**, *496*, 110.
19. Chrzanowski, W.; Wieckowski, A. *Langmuir* **1997**, *13*, 5974.
20. Chrzanowski, W.; Wieckowski, A. *Catal. Lett.* **1998**, *50*, 69.
21. Waszczuk, P.; Solla-Gullon, J.; Kim, H. S.; Tong, Y. Y.; Montiel, V.; Aldaz, A.; Wieckowski, A. *J. Catal.* **2001**, *203*, 1.
22. Iwasita, T. *Electrochimca Acta* **2002**, *47*, 3663.
23. Bock, C.; Paquet, C.; Couillard, M.; Botton, G. A.; MacDougall, B. R. *J. Am. Chem. Soc.* **2004**, *126*, 8028.
24. Jang, J. H.; Han, S.; Hyeon, T.; Oh, S. M. *J. Power Source* **2003**, *123*, 79.
25. Rodriguez, N. M.; Chambers, A.; Baker, R. T. K. *Langmuir* **1995**, *11*, 3862.
26. Yoon, S.-H.; Lim, S.; Hong, S.-H. *Carbon* **2005**, *43*, 1828.
27. Kim, T. G.; Lim, Y.; Kwon, K. H.; Hong, S. H.; Qiao, W. M.; Rhee, C. K.; Yoon, S.-H.; Mochida, I. *Langmuir* **2006**, *22*, 9086.
28. Vericat, C.; Wakisaka, M.; Haasch, R.; Bagus, P. S.; Wieckowski, A. *J. Solid State Electrochem.* **2004**, *8*, 794.
29. Kim, H.; Park, J.-N.; Lee, W.-H. *Catal. Today* **2003**, *87*, 237.
30. Folkesson, B. *Acta Chemica Scandinavica* **1973**, *27*, 287.
31. Briggs, D.; Seah, M. P. *Practical Surface Analysis by Auger and X-ray Photoelectron Spectroscopy*; John Wiley and Sons: 1990; Vol. 1.
32. Mayrhofer, K. J. J.; Blizanac, B. B.; Arenz, M.; Stamenkovic, V. R.; Ross, P. N.; Markovic, N. M. *J. Phys. Chem. B* **2005**, *109*, 14433.
33. Iwasita, T. In *Methanol and CO Electrooxidation*; Vielstich, W., Lamm, A., Gasteiger, H. A., Eds.; John Wiley and Sons: 2003; Vol. 2, pp 603-624.